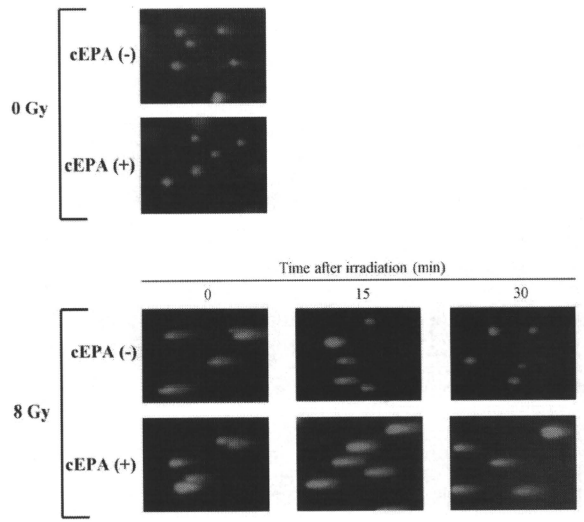

Figure 3. Detection of DNA damage in HCT116 cells by combining cEPA and X-ray radiation. Human colon carcinoma HCT116 cells were incubated with or without 30 μM cEPA for 30 min, and then the plates were radiated with 8 Gy X-ray. After irradiated cells with or without cEPA were harvested at 0, 15 and 30 min, the cells were lysed in neutral buffer, electophoresed and stained following the manufacturer's instructions. The stained cells are shown by x400 magnification under a fluorescent microscope.

Effect of cEPA on survival of HCT116 cell radiosensitivity. To determine whether cEPA enhances cellular sensitivity to X-ray radiation, the HCT116 cell line was cultured receiving the combined cEPA/radiation treatment, and then clonogenic survival analysis was performed. HCT116 cells were treated with 1% DMSO (vehicle control) or 30 μM cEPA for 48 h with 8 Gy of radiation 0, 24 or 48 h after treatment of cEPA [(a), (b) or (c) in Fig. 4A, respectively], and subsequently plated in 100-mm dishes at different densities based on the stringency of treatments. This protocol was used in an attempt to eliminate any effects of trypsinization on post-irradiation signaling/recovery processes. The surviving fractions obtained after 30 μM cEPA treatment only and 8 Gy X-ray radiation exposure only were 0.89±0.08 and 0.12±0.01 for HCT116 cells, respectively. As shown in Fig. 4B, cEPA exposure for 48 h after irradiation [i.e., 'post-irradiation' = (a) of Fig. 4A] resulted in an increase in radiation-induced cell killing for HCT116 cells, and the surviving fraction was 0.017±0.002; therefore, the survival rate of radiosensitive enhancement was >7. Furthermore, treatment combining cEPA with radiation therapy was enhanced with the cEPA dose, and 40 μM cEPA showed an approximately 10-fold reduction in clonogenic survival compared with the control (0 μM cEPA) (Fig. 4C). In this treatment protocol, when cEPA was treated for 48 h with radiation 24 or 48 h after cEPA treatment ['mid-irradiation' = (b) or 'pre-irradiation' = (c) in Fig. 4A, respectively], the radiosensitizing effect had no influence compared with no treatment with cEPA. These data indicate that radiosensitization induced by cEPA is mediated through a post-irradiation process or event.

Effect of cEPA on enhancement of radiation-induced apoptosis. X-ray radiation is known to be a strong inducer of apoptosis (33). To examine whether susceptibility to apoptosis can be a determinant of cEPA treatment, the effect of cEPA on radiation-induced apoptosis in HCT116 cells was investigated using flow cytometry. In this experiment, the three combinations of 30 μM cEPA and 8 Gy X-ray irradiation were the same schedules as in Fig. 4A (a-c). After cells were treated with cEPA for 48 h with irradiation, flow cytometric analysis was performed instead of the clonogenic assay in Fig. 4A. As shown in Fig. 5, a lower concentration of cEPA (i.e., 30 μM of the LD_{50} value of HCT116 cell growth in Fig. 2A) alone did not induce apoptosis, although apoptotic cells were induced by 8 Gy X-ray radiation. Radiation-induced apoptosis depended on the incubation time after irradiation, and cells incubated for 48 h after irradiation [i.e., (a) of Fig. 4A] showed the highest apoptosis induction compared with other cells incubated for 24 and 0 h after irradiation; i.e., (b) and (c) of Fig. 4A. In HCT116 cells, DNA damage occurred immediately with irradiation (Fig. 3), although apoptosis was induced 24 h or later after irradiation. The apoptotic level in cultures receiving combined radiation/cEPA treatment was greater than in the radiation-only group; therefore, the cEPA-mediated increase in radiosensitivity could be attributed to enhanced susceptibility to apoptosis.

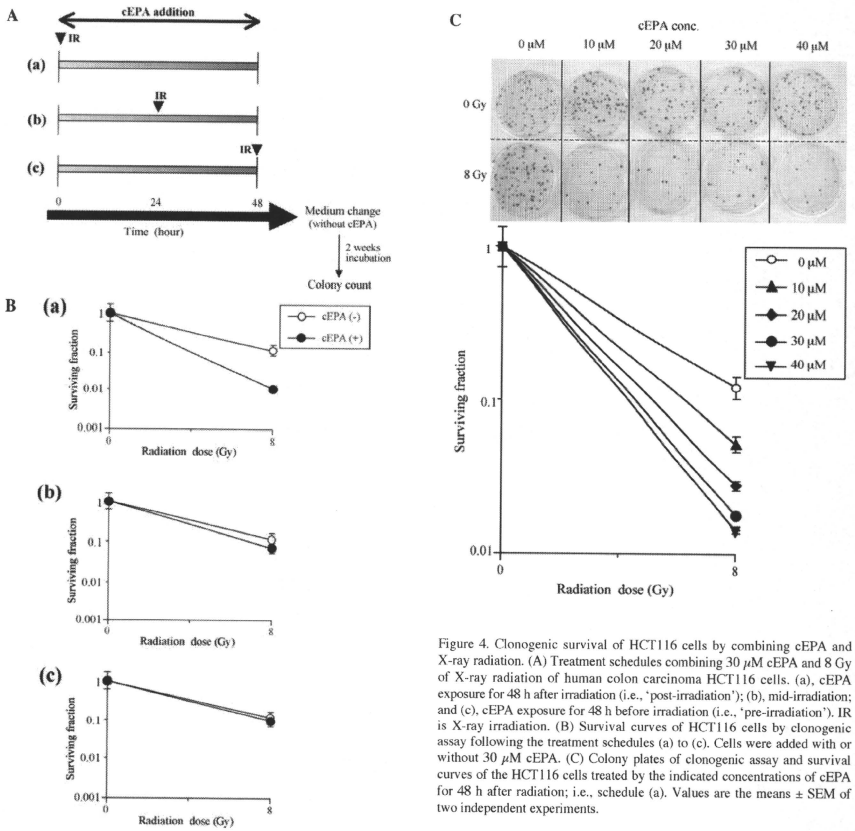

Figure 4. Clonogenic survival of HCT116 cells by combining cEPA and X-ray radiation. (A) Treatment schedules combining 30 μM cEPA and 8 Gy of X-ray radiation of human colon carcinoma HCT116 cells. (a), cEPA exposure for 48 h after irradiation (i.e., 'post-irradiation'); (b), mid-irradiation; and (c), cEPA exposure for 48 h before irradiation (i.e., 'pre-irradiation'). IR is X-ray irradiation. (B) Survival curves of HCT116 cells by clonogenic assay following the treatment schedules (a) to (c). Cells were added with or without 30 μM cEPA. (C) Colony plates of clonogenic assay and survival curves of the HCT116 cells treated by the indicated concentrations of cEPA for 48 h after radiation; i.e., schedule (a). Values are the means ± SEM of two independent experiments.

Discussion

We reported previously that conjugated PUFA, such as cEPA prepared by alkaline treatment of PUFA, was a two-fold stronger pol inhibitor than normal PUFA (31). cEPA did not influence pol activities from plants and prokaryotes and other DNA metabolic enzyme activities, and no interaction of cEPA with DNA was detected in an independent DNA-binding assay (i.e., Tm of double-stranded DNA measurements) (23). These results suggested that selective inhibitory action by cEPA might be due to specific binding to pol enzymes. Furthermore, the mechanisms by which cEPA suppresses human cancer cell growth were investigated, and it was revealed that the inhibition of pol activity by cEPA influenced not only cell proliferation but also the cell cycle (31). Cell cycle arrest in the G1 phase by cEPA was considered to be induced by the p53/p21 pathway from the ATR-Chk1/2-signaling pathway in HCT116 cells (16). Since cEPA did not influence the proliferation of normal cells (data not shown), cEPA should also be considered the lead compound of a group of potentially useful agents for cancer chemotherapy.

In this study, cEPA (conjugated C20:5 fatty acid) was prepared from EPA by alkaline treatment, as described in Materials and methods, and the chemically synthesized fraction was used. This fraction contained 98% cEPA, which had conjugated double bonds, but did not contain hydroperoxy- and/or hydroxy-fatty acids (data not shown); however, each cEPA isomer, which has a *cis*- or *trans*-double bond compound, was not separated and purified. Jain *et al* reported that *trans*-arachidonic acid (C20:4 fatty acid) isomers (especially 5,6- *trans*-arachidonic acid) showed distinct activity by targeting cell progression through the cell cycle (arrest in the G1 phase) and inducing apoptosis (34).

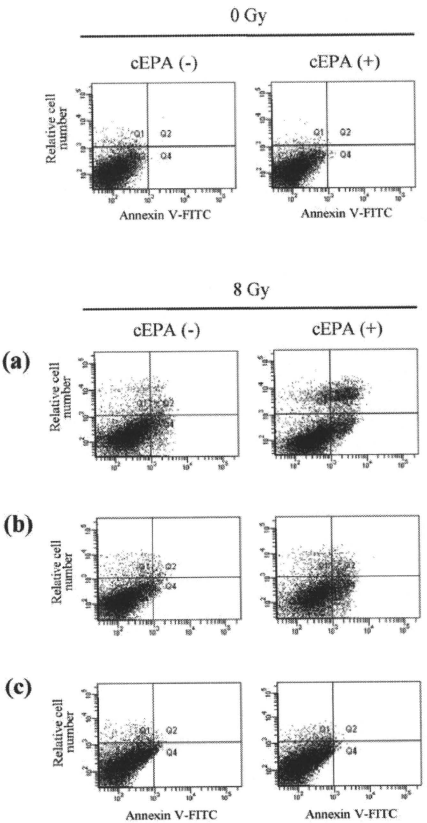

Figure 5. Detection of apoptosis in HCT116 cells by combining cEPA and X-ray radiation. Treatment schedules (a) to (c) combining 30 μM cEPA and 8 Gy X-ray radiation of human colon carcinoma HCT116 cells are shown in Fig. 4A. Treated cells were cultured for 48 h, harvested, stained with annexin V, and then analyzed using flow cytometry.

These results suggested that the *trans*-cEPA isomer in the fraction might have bio-activities, such as pol inhibition, prevention of cancer cell growth, G1 phase arrest of the cancer cell cycle, and apoptosis induction.

Radiotherapy remains a primary cancer treatment modality for solid tumors, and the ability to enhance its efficacy is thus likely to impact a significant number of cancer patients. DNA repair-related pols, especially pol ß, have been shown to be altered in around 30% of tumors, suggesting a role in tumor formation (35). These changes include overexpression, truncation and mutations modulating the activity of these enzymes and are postulated to influence DNA repair and therefore possibly tumorigenesis (36-38). This is the initial investigation into the combination of radiation and cEPA, which is a selective mammalian pol inhibitor. The results of this study indicate that cEPA enhanced the radiosensitivity of human colon carcinoma HCT116 cells, which inhibited the activities of pols in the cells (Fig. 1), reduced the expression of pols, especially DNA repair-related pols such as pols ß, δ and ε (Fig. 2), and caused consequent DNA repair inactivation of damaged DNA, including DSBs by X-ray irradiation (Fig. 3). Furthermore, the cell treatment of post-irradiation addition of cEPA showed significantly greater anticancer effects, such as inductions of cancer cell killing and apoptosis, than other combined cEPA/radiation schedules (Figs. 4 and 5). In conclusion, combining selective inhibitors of DNA repair-related pols, such as cEPA, and radiation might have clinical potential as a cancer treatment strategy.

Acknowledgments

This work was supported in part by the Academic Frontier Project for Private Universities: matching fund subsidy from the Ministry of Education, Science, Sports and Culture of Japan (MEXT), 2006-2010, (H.Y. and Y.M.). Y.Y. acknowledges a Grant-in-Aid for Young Scientists (B) (no. 21780136) from MEXT. Y.M. acknowledges a Grant-in-Aid for Young Scientists (A) (no. 19680031) from MEXT, and The Salt Science Research Foundation, No. 09S3 (Japan).

References

1. Kornberg A and Baker TA: DNA replication. 2nd edition. W.D. Freeman and Co., New York, pp197-225, 1992.
2. Hubscher U, Maga G and Spadari S: Eukaryotic DNA polymerases. Annu Rev Biochem 71: 133-163, 2002.
3. Friedberg EC, Feaver WJ and Gerlach VL: The many faces of DNA polymerases: strategies for mutagenesis and for mutational avoidance. Proc Natl Acad Sci USA 97: 5681-5683, 2000.
4. Takata K, Shimizu T, Iwai S and Wood RD: Human DNA polymerase N (POLN) is a low fidelity enzyme capable of error-free bypass of 5S-thymine glycol. J Biol Chem 281: 23445-23455, 2006.
5. Sakaguchi K, Sugawara F and Mizushina Y: Inhibitors of eukaryotic DNA polymerases. Seikagaku 74: 244-251, 2002.
6. Mizushina Y: Specific inhibitors of mammalian DNA polymerase species. Biosci Biotechnol Biochem 73: 1239-1251, 2009.
7. Mizushina Y, Tanaka N, Yagi H, Kurosawa T, Onoue M, Seto H, Horie T, Aoyagi N, Yamaoka M, Matsukage A, Yoshida S and Sakaguchi K: Fatty acids selectively inhibit eukaryotic DNA polymerase activities in vitro. Biochim Biophys Acta 1308: 256-262, 1996.
8. Mizushina Y, Yoshida S, Matsukage A and Sakaguchi K: The inhibitory action of fatty acids on DNA polymerase ß. Biochim Biophys Acta 1336: 509-521, 1997.
9. Iigo M, Nakagawa T, Iwahori Y, Asamoto M, Yazawa K, Araki E and Tsuda H: Inhibitory effects of docosahexaenoic acid on colon carcinoma 26 metastasis to the lung. Br J Cancer 75: 650-655, 1997.
10. Iwamoto S, Senzaki H, Kiyozuka Y, Ogura E, Takada H, Hioki K and Tsubura A: Effects of fatty acids on liver metastasis of ACL15 rat colon cancer cells. Nutr Cancer 31: 143-150, 1998.
11. Lopez A and Gerwick WH: Two new icosapentaenoic acids from the temperate red seaweed *Ptilota filicina* J. Agardh. Lipids 22: 190-194, 1987.
12. Mikhailova MV, Bemis DL, Wise ML, Gerwick WH, Norris JN and Jacobs RS: Structure and biosynthesis of novel conjugated polyene fatty acids from the marine green alga *Anadyomene stellata*. Lipids 30: 583-589, 1995.
13. Shultz TD, Chew BP, Seaman WR and Luedecke LO: Inhibitory effect of conjugated dienoic derivatives of linoleic acid and ß-carotene on the in vitro growth of human cancer cells. Cancer Lett 63: 125-133, 1992.
14. Kelly GS: Conjugated linoleic acid: a review. Altern Med Rev 6: 367-382, 2001.
15. Yonezawa Y, Tsuzuki T, Eitsuka T, Miyazawa T, Hada T, Uryu K, Murakami-Nakai C, Ikawa H, Kuriyama I, Takemura M, Oshige M, Yoshida H, Sakaguchi K and Mizushina Y: Inhibitory effect of conjugated eicosapentaenoic acid on human DNA topoisomerases I and II. Arch Biochem Biophys 435: 197-206, 2005.
16. Yonezawa Y, Hada T, Uryu K, Tsuzuki T, Nakagawa K, Miyazawa T, Yoshida H and Mizushina Y: Mechanism of cell cycle arrest and apoptosis induction by conjugated eicosapentaenoic acid, which is a mammalian DNA polymerase and topoisomerase inhibitor. Int J Oncol 30: 1197-1204, 2007.
17. Yonezawa YK, Sasaki R, Ota Y, Suzuki Y, Fukushima S, Hada T, Uryu K, Sugimura K, Yoshida H and Mizushina Y: Cell cycle arrest triggered by conjugated eicosapentaenoic acid occurs through several mechanisms including G1 checkpoint activation by induced RPA and ATR expression. Biochim Biophys Acta 1790: 339-346, 2009.
18. Haimovitz-Friedman A: Radiation-induced signal transduction and stress response. Radiat Res 150: 102-108, 1998
19. Garcia-Barros M, Paris F, Cordon-Cardo C, Lyden D, Rafii S, Haimovitz-Friedman A, Fuks Z and Kolesnick R: Tumor response to radiotherapy regulated by endothelial cell apoptosis. Science 300: 1155-1159, 2003.
20. Paris F, Fuks Z, Kang A, Capodieci P, Juan G, Ehleiter D, Haimovitz-Friedman A, Cordon-Cardo C and Kolesnick R: Endothelial apoptosis as the primary lesion initiating intestinal radiation damage in mice. Science 293: 293-297, 2001.
21. Li Y, Carty MP, Oakley GG, Seidman MM, Medvedovic M and Dixon K: Expression of ATM in ataxia telangiectasia fibroblasts rescues defects in DNA double-strand break repair in nuclear extracts. Environ Mol Mutagen 37: 128-140, 2001.
22. El-Awady RA, Dikomey E and Dahm-Daphi J: Radiosensitivity of human tumour cells is correlated with the induction but not with the repair of DNA double-strand breaks. Br J Cancer 89: 593-601, 2003.
23. Sakata K, Someya M, Matsumoto Y and Hareyama M: Ability to repair DNA double-strand breaks related to cancer susceptibility and radiosensitivity. Radiat Med 25: 433-438, 2007.
24. Shiloh Y: ATM and related protein kinases: safeguarding genome integrity. Nat Rev Cancer 3: 155-168, 2003.
25. Shiloh Y and Lehmann AR: Maintaining integrity. Nat Cell Biol 6: 923-928, 2004.
26. Association of Official Analytical Chemists: Acids (poly-unsaturated) in oil and fats. In: Official Methods of Analysis of the Association of Official Analytical Chemists. Helrich K (ed). Association of Official Analytical Chemists, Arlington, pp960-963, 1990.
27. Pitt GAJ and Morton RA: Ultra-violet spectrophotometry of fatty acids. Prog Chem Fats Other Lipids 4: 227-278, 1957.
28. Mosmann T: Rapid colorimetric assay for cellular growth and survival: application to proliferation and cytotoxicity assays. J Immunol Methods 65: 55-63, 1983.
29. Heintel D, Kroemer E, Kienle D, Schwarzinger I, Gleiss A, Schwarzmeier J, Marculescu R, Le T, Mannhalter C, Gaiger A, Stilgenbauer S, Dohner H, Fonatsch C and Jager U: German CLL Study Group. High expression of activation-induced cytidine deaminase (AID) mRNA is associated with unmutated IGVH gene status and unfavourable cytogenetic aberrations in patients with chronic lymphocytic leukaemia. Leukemia 18: 756-762, 2004.
30. Singh NP, McCoy MT, Tice RR and Schneider EL: A simple technique for quantitation of low levels of DNA damage in individual cells. Exp Cell Res 175: 184-191, 1998.
31. Yonezawa Y, Hada T, Uryu K, Tsuzuki T, Eitsuka T, Miyazawa T, Murakami-Nakai C, Yoshida H and Mizushina Y: Inhibitory effect of conjugated eicosapentaenoic acid on mammalian DNA polymerase and topoisomerase activities and human cancer cell proliferation. Biochem Pharmacol 70: 453-460, 2005.
32. Rogakou EP, Pilch DR, Orr AH, Ivanova VS and Bonner WM: DNA double-stranded breaks induce histone H2AX phosphorylation on serine 139. J Biol Chem 273: 5858-5868, 1998.
33. Blumenstein M, Hossfeld DK and Dührsen U: Indirect radiation leukemogenesis in DBA/2 mice: increased expression of B2 repeats in FDC-P1 cells transformed by intracisternal A-particle transposition. Ann Hematol 76: 53-60, 1998.
34. Jain K, Roy U, Ardelt B, Krishna UM, Falck JR, Pozarowski P, Kunicki J, Darzynkiewicz Z and Balazy M: 5E, 8Z, 11Z, 14Z-eicosatetraenoic acid, a novel trans isomer of arachidonic acid, causes G1 phase arrest and induces apoptosis of HL-60 cells. Int J Oncol 27: 1177-1185, 2005.
35. Albertella MR, Lau A and O'Connor MJ: The overexpression of specialized DNA polymerases in cancer. DNA Repair (Amst) 4: 583-593, 2005.
36. Lang T, Maitra M, Starcevic D, Li SX and Sweasy JB: A DNA polymerase ß mutant from colon cancer cells induces mutations. Proc Natl Acad Sci USA 101: 6074-6079, 2004.
37. Starcevic D, Dalal S and Sweasy JB: Is there a link between DNA polymerase ß and cancer? Cell Cycle 3: 998-1001, 2004.
38. Sweasy JB, Lang T, Starcevic D, Sun KW, Lai CC, Dimaio D and Dalal S: Expression of DNA polymerase {beta} cancer-associated variants in mouse cells results in cellular transformation. Proc Natl Acad Sci USA 102: 14350-14355, 2005.

ORIGINAL ARTICLE

NUCLEAR FACTOR-κB EXPRESSION AS A NOVEL MARKER OF RADIORESISTANCE IN EARLY-STAGE LARYNGEAL CANCER

Kenji Yoshida, MD,[1] Ryohei Sasaki, MD, PhD,[1] Hideki Nishimura, MD, PhD,[1] Yoshiaki Okamoto, MD, PhD,[1] Yoko Suzuki, MS,[1] Tetsuya Kawabe, MD, PhD,[1] Miki Saito, MD, PhD,[2] Naoki Otsuki, MD, PhD,[2] Yoshitake Hayashi, MD, PhD,[3] Toshinori Soejima, MD, PhD,[4] Kenichi Nibu, MD, PhD,[2] Kazuro Sugimura, MD, PhD[5]

[1] Division of Radiation Oncology, Kobe University Graduate School of Medicine, Hyogo, Japan. E-mail: rsasaki@med.kobe-u.ac.jp
[2] Department of Otolaryngology-Head and Neck Surgery, Kobe University Graduate School of Medicine, Hyogo, Japan
[3] Department of Pathology, Kobe University Graduate School of Medicine, Hyogo, Japan
[4] Department of Radiation Oncology, Hyogo Cancer Center, Hyogo, Japan
[5] Department of Radiology, Kobe University Graduate School of Medicine, Hyogo, Japan

Accepted 16 July 2009
Published online 2 November 2009 in Wiley InterScience (www.interscience.wiley.com). DOI: 10.1002/hed.21239

Abstract: *Background.* The aim of this study was to evaluate the significance of nuclear factor-kappa B (NF-κB) expression as a marker of radioresistance in early-stage laryngeal cancer.

Methods. Thirty-five patients with local recurrence and 70 case-matched patients without local recurrence were entered in this study. NF-κB expression was compared with Bcl-2 and epidermal growth factor (EGF) receptor expression by immunohistochemistry, using pretreatment biopsy specimens. The prognostic value of NF-κB was also evaluated. Twenty-nine recurrent tumors were compared with pretreatment tumors.

Results. NF-κB expression in pretreatment tumors significantly correlated with local tumor control ($p = .01$), but bcl-2 and EGF receptor expression did not. Only NF-κB expression showed prognostic significance for local tumor control in both univariate and multivariate analyses ($p = .008$ and .04, respectively). NF-κB expression was markedly enhanced in 23 of 29 (80%) recurrent tumors.

Conclusion. NF-κB expression may be a novel marker of radioresistance in early-stage laryngeal cancer. © 2009 Wiley Periodicals, Inc. *Head Neck* **32:** 646–655, 2010

Keywords: early-stage laryngeal cancer; nuclear factor-κB; radioresistance; radiotherapy; immunohistochemistry

Correspondence to: R. Sasaki

Contract grant sponsor: The Shinryokukai, Kobe, Japan; contract grant sponsor: Hyogo Science and Technology Association Japan; contract grant sponsor: Japan Food Chemical Research Foundation; contract grant sponsor: Scientific Research of the Ministry of Education, Culture, Sports, Science and Technology, Japan; contract grant numbers: Grants-in-Aid 17790859, 17501269, 17591268, 20890127, and 21249066.

This study was presented at the 49th Annual Meeting of the American Society for Therapeutic Radiology and Oncology (ASTRO), October 28 to November 1, 2007, in Los Angeles, CA; at the 14th European Cancer Conference (ECCO14), September 23–27, 2007, in Barcelona, Spain; and at the 21st Annual Meeting of the Japanese Society for Therapeutic Radiology and Oncology (JASTRO), October 16–18, 2008, in Sapporo, Japan.

The content of this study was selected for a Scientific Award at the 45th Annual Meeting of the Japanese Society of Clinical Oncology (JSCO), October 30 to November 1, 2008, in Nagoya, Japan.

Head and neck cancers, which are often caused by cigarette smoke, are the sixth most prevalent cancers in the world, with a global incidence of

approximately 500,000 cases per year.[1] Laryngeal cancers are dominated by squamous cell carcinomas, of which 67% arise in the glottic region, 31% in the supraglottis, and 2% in the subglottis.[2] Treatment options for T1–T2N0 classification laryngeal cancers include transoral laser excision, radiotherapy, and open partial laryngectomy. Treatment goals include cure, laryngeal voice preservation, improvement in voice quality, optimization of swallowing, and minimization of xerostomia.[3] Local control rates and voice quality are comparable for patients treated with transoral laser excision and radiotherapy, but open partial laryngectomy leads to poorer voice quality.[4–9] At our institution, we use radiotherapy as an initial treatment for early-stage laryngeal cancer and reserve salvage surgery for tumor recurrences.

Although most patients with early-stage laryngeal cancer can be cured with radiotherapy, these outcomes have not improved over the past 2 decades, in part because there are no clinicopathological features that can consistently identify radioresistant tumors.[10–12] Assessments of biological markers, such as p53, bcl-2, vascular endothelial growth factor (VEGF), and epidermal growth factor (EGF) receptor, may provide new insights into the treatment of early-stage laryngeal cancer.[13–17] Nix et al[14] reported a correlation between the bcl family and poor local control in early-stage laryngeal cancer. Demiral et al[15] reported a correlation between EGF receptor expression and poor local control in early-stage laryngeal cancer. However, because few reports exist on how those factors affect local disease controllability,[17] new biological markers are required.

Nuclear factor-kappa B (NF-κB) is an inducible transcription factor that has been shown to be associated with the origin and progression of cancer by controlling the expression of genes involved in cell growth, apoptosis, adhesion, and migration.[18] NF-κB includes subunits, known as p50, p52, p65 (RelA), RelB, and c-Rel, that are able to form either homodimers or heterodimers.[19] The inactive form of NF-κB is localized in the cytoplasm bound to an inhibitor IκB. Once released from the inhibitory molecule, NF-κB is translocated to the nucleus, where it can bind to target sites in DNA and can regulate transcription of certain genes.[20] The best-characterized subunit of NF-κB is p65 (RelA), which forms NF-κB heterodimers together with p50 through the classical pathway. The heterodimers are potent activators of gene expression, and p65 (RelA) is responsible for this activation.[21,22] Thus, NF-κB/p65 is thought to play important roles in carcinogenesis or resistance to anticancer therapy. Recently, the RelB/p52 NF-κB heterodimer, which forms through the nonclassical pathway, has been newly recognized as an activator of gene expression.[23] In a clinical study, Izzo et al[23] demonstrated that activated NF-κB had predictive value for tumor controllability after neoadjuvant chemoradiotherapy in patients with esophageal cancer. However, it is unclear whether NF-κB activation predicts local tumor controllability of early-stage laryngeal cancer treated with radiotherapy as a single modality.[24]

In this study, we first evaluated NF-κB expression by immunohistochemistry using pretreatment biopsy specimens compared with bcl-2 and EGF receptor expression. Next, we investigated whether NF-κB expression had a prognostic ability for local tumor control in patients with early-stage laryngeal cancer. Moreover, NF-κB expression in recurrent tumors was evaluated and compared with the respective pretreatment tumors.

MATERIALS AND METHODS

Patients. Between 1990 and 2005, 250 patients with biopsy-proven squamous cell carcinoma of the larynx (T1–T2N0M0 classification) were treated by definitive radiotherapy at Kobe University Hospital. Of these 250 patients, 48 patients experienced local recurrence. Among these 48 patients, 35 could be evaluated with immunohistochemical analysis using their pretreatment biopsy specimens. Subsequently, to minimize confounding variables, patients without local recurrence were selected to be matched with patients with local recurrence as much as possible to establish a 1-to-2 matching. The matching factors were age, sex, smoking history (Brinkman Index), tumor stage, histological grade, radiation dose, radiation method, and overall treatment time (OTT). Finally, 35 patients with local recurrence and 70 patients without local recurrence were enrolled in this study. Patients with local recurrence constituted the "radioresistant group," and patients without local recurrence constituted the "radiosensitive group." Staging was performed according to

Table 1. Patient, tumor, and treatment details of radioresistant and radiosensitive groups ($n = 105$).

Characteristic	Radioresistant group ($n = 35$)	Radiosensitive group ($n = 70$)	p value
Age, y			
≤60	6	12	.78
>60	29	58	
Median (range)	67 (46–85)	68 (48–83)	
Sex			
Male	32	65	.90
Female	3	5	
Smoking (Brinkman Index)			
≤600	7	12	.21
>600	26	45	
Not available	2	13	
Median (range)	1200 (0–3000)	960 (08–2600)	
Tumor location			
Glottic	25	63	.03
Nonglottic	10	7	
Tumor classification			
T1	18	49	.10
T2	17	21	
Histology			
Well-differentiated SCC	7	22	.60
Moderately differentiated SCC	10	18	
Poorly differentiated SCC	2	2	
SCC, NOS	16	28	
Radiation dose, Gy			
≤66	15	42	0.15
>66	20	28	
Median (range)	70 (56–76.8)	66 (60–74.4)	
Radiation method			
Once daily	30	60	.78
Twice daily	5	10	
OTT, d			
≤45	12	29	.62
>45	23	41	
Median (range)	48 (35–59)	47 (37–73)	

Abbreviations: SCC, squamous cell carcinoma; NOS, not otherwise specified; OTT, Overall treatment time.

TNM classification of the Union Internationale Contre le Cancer (UICC 1997). The details of patient and tumor characteristics in these 2 groups are shown in Table 1.

Radiotherapy. All patients were treated with external-beam radiotherapy using high-energy photons from a 4-MV X-ray linear accelerator. Patients were immobilized with a thermoplastic mask, and CT images were acquired in the treatment position to allow for 3-dimensional treatment planning. Typically, a parallel-opposed field was used, and no elective irradiation for neck lymph nodes was performed. The median total doses of the radioresistant and radiosensitive groups were 70 Gray (Gy) (range, 56–76.8) and 66 Gy (range, 60–74.4), respectively. In the radioresistant group, 30 patients (86%) were treated once daily (2 Gy per fraction), with the total dose ranging from 56 to 70 Gy, and 5 patients (14%) were treated twice daily (1.2 Gy per fraction at 6-hour intervals), with the total dose ranging from 72 to 76.8 Gy. In the radiosensitive group, 60 patients (86%) were treated once daily, with the total dose ranging from 60 to 70 Gy, and 10 patients (14%) were treated twice daily, with the total dose ranging from 72 to 74.4 Gy. The median OTTs of each group were 48 days (range, 35–59) and 47 days (range, 37–73), respectively. Details of the radiotherapy are also shown in Table 1.

Immunohistochemistry. Immunohistochemical evaluation was performed for 105 patients with pretreatment specimens using the following procedures. Four-micrometer-thick sections from formalin-fixed, paraffin-embedded tissue blocks were placed on poly-L-lysine–coated slides and

dried for 2 hours at 60°C. Immunohistochemical staining of NF-κB p65, bcl-2, and EGF receptor was performed with the Dako Envision Plus System (Dako A/S, Copenhagen, Denmark) following the manufacturer's instructions. Briefly, the sections were deparaffinized in xylene and rehydrated in graded ethanol. Endogenous peroxidase activity was blocked using a 0.3% solution of hydrogen peroxidase in Tris-buffered saline (TBS) at room temperature for 10 minutes. A few drops of the diluted normal blocking serum were placed on the tissue, which was incubated at room temperature for 10 minutes. The sections were then incubated at 4°C overnight with primary monoclonal antibodies for NF-κB p65 (1:500), bcl-2 (1:150), and EGF receptor (1:150) (Santa Cruz Biotechnology, Santa Cruz, CA). The next day, the sections were rinsed 3 times with TBS for 5 minutes each and then incubated for 60 minutes with secondary antibody. Peroxidase activity was visualized with 0.03% 3,3′-diaminobenzidine tetrahydrochloride (DAB) solution for 10 minutes. After being counterstained with hematoxylin and rinsed in deionized water, the sections were mounted.

NF-κB expression was evaluated on the basis of staining intensity and extent according to the criteria of Ross and colleagues.[25] The intensities of cytoplasmic and/or nuclear staining were graded as weak, moderate, or intense. The staining extents were also graded as focal (≤10%), regional (11% to 50%), or diffuse (>50%). Specimens graded as moderate regional, moderate diffuse, intense regional, and intense diffuse were considered positive (see Figure 1). Briefly, a specimen that demonstrated >10% of tumor cells with moderate to intense staining was considered positive. Bcl-2 and EGF receptor expression levels were evaluated with the same criteria as those for cytoplasmic staining. Specimens of recurrent tumors from 29 patients were also evaluated and compared with their corresponding pretreatment tumors for NF-κB expression.

Statistics. Statistical analyses were performed using Sigma Plot 9.0 software (Systat Corporation, San Jose, CA). The chi-square test was performed to assess measures of association in a grouped frequency table. Local control rates were drawn using the Kaplan–Meier method and compared with use of the log-rank test. The follow-up duration of local control rates was calculated from the start of treatment. To identify prognostic factors for local tumor control, univariate analysis was first performed using the log-rank test. Multivariate analysis was performed on statistically significant variables identified in the univariate analysis using a Cox proportional hazards regression model that yields adjusted hazard ratios (HRs) and 95% confidence intervals (CIs). A value of $p < .05$ was considered statistically significant.

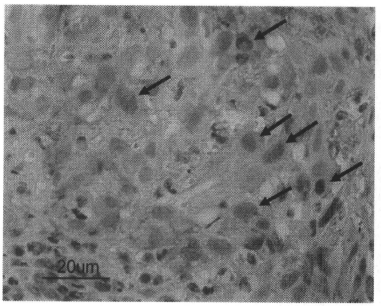

FIGURE 1. A representation of positive NF-κB expression (52 years old, male, T2 glottic cancer). Note that both cytoplasmic staining and nuclear staining were observed. Arrowheads indicate the stained nucleus. NF, nuclear factor.

RESULTS

Correlation Between Local Tumor Control and NF-κB, bcl-2, and EGF Receptor Expression. The result of immunohistochemical analysis of NF-κB expression was predominantly cytoplasmic NF-κB expression, with or without scattered nuclear NF-κB expression. There were no cases that showed only nuclear expression without cytoplasmic expression. Therefore, combined cytoplasmic and nuclear (whole) NF-κB expression was used for the analyses as NF-κB expression. Sixty-two of 105 patients were determined as positive for NF-κB expression. Among the 35 specimens from the radioresistant group, 27 (77%) were positive, and 8 (23%) were negative, whereas among the 70 specimens of the radiosensitive group, 35 (50%) were positive, and 35 (50%) were negative. NF-κB expression significantly correlated with local tumor recurrence ($p = .01$), whereas bcl-2 and EGF receptor expression did not ($p = .75$ and .48, respectively) (Table 2). Positive predictive values (PPVs) for

Table 2. Analyses of NF-κB, bcl-2, and EGF receptor expressions in pretreatment tumors.

	Total (n = 105)	Radioresistant group (n = 35)	Radiosensitive group (n = 70)	p value	PPV
Single factor					
NF-κB					
Positive	62	27	35	.01	0.44
Negative	43	8	35		
Bcl-2					
Positive	93	31	62	.75	0.35
Negative	12	4	8		
EGF receptor					
Positive	78	28	50	.48	0.42
Negative	27	7	20		
Combined factors					
NF-κB and bcl-2					
Positive	59	25	35	.06	0.42
Negative	45	10	35		
NF-κB and EGF receptor					
Positive	58	23	35	.19	0.40
Negative	47	12	35		
NF-κB, bcl-2, and EGF receptor					
Positive	57	22	35	.30	0.39
Negative	48	13	35		

Abbreviations: NF-κB, nuclear factor-kappa B; EGF receptor, epidermal growth factor receptor; PPV, positive predictive value.

NF-κB, bcl-2, and EGF receptor were 0.44, 0.35, and 0.42, respectively. Subsequently, we assessed whether any combination with other biological markers might improve PPV. The PPVs of NF-κB and bcl-2, NF-κB and EGF receptor, and a combination of NF-κB, bcl-2, and EGF receptor were 0.42, 0.40, and 0.39, respectively (Table 2). The median duration to relapse of the 27 NF-κB positive cases was 11 months (range, 4–36), with a median follow-up of 60 months (range, 19–192), whereas that of the 8 NF-κB negative cases was 8 months (range, 3–23), with a median follow-up of 57 months (range, 15–156). Additionally, evaluation of the nuclear NF-κB expression was performed separately. Twenty-six of 105 specimens were determined to be positive for nuclear NF-κB expression. Among the 35 specimens from the radioresistant group, 14 (40%) were positive, and 21 (60%) were negative, whereas among the 70 specimens from the radiosensitive group, 12 (17%) were positive, and 58 (83%) were negative. Nuclear NF-κB expression also significantly correlated with local recurrence (p = .02) with a PPV of 0.54, but it did not show stronger expression. PPV was also not remarkably changed.

The 5-year local control rate in patients with positive NF-κB expression was significantly worse than that in patients with negative NF-κB expression (46% and 81%, respectively, p = .008) (Figure 2A), but there were no differences regarding local control rates when cases were classified according to bcl-2 or EGF receptor expression (p = .86 and .55, respectively) (Figures 2B and 2C). The 5-year local control rate in patients with positive nuclear NF-κB expression was also significantly worse than that in patients with negative nuclear NF-κB expression (40% and 70%, respectively, p = .02).

Prognostic Factors for Local Tumor Control. Clinical factors, including age, tumor location, tumor stage, radiation dose, OTT, and Brinkman Index, were also tested in addition to biological markers. NF-κB expression was evaluated as a single variable because there was a strong "positive" correlation in local control between whole and nuclear NF-κB expression from the previous results. In univariate analysis, NF-κB expression was a significant prognostic factor for local tumor control (p = .008), as were tumor location and T classification (p = .02, and .03, respectively; Table 3). In multivariate analysis with those 3 factors, only NF-κB expression maintained prognostic significance (p = .04, HR = 0.43, 95% CI = 0.18–0.99; Table 3).

Comparison of NF-κB Expression Between Recurrent and Pretreatment Tumors. Among the 35 patients in the radioresistant group with

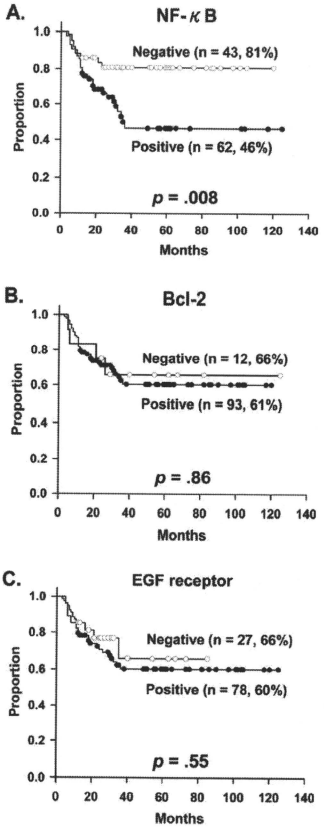

FIGURE 2. (**A**) Five-year local control rates among 105 patients selected for case-matched analysis according to NF-κB expression (positive cases: 46%; negative cases: 81%). (**B**) Five-year local control rates according to Bcl-2 expression (positive cases: 61%; negative cases: 66%). (**C**) Five-year local control rates according to EGF receptor expression (positive cases: 60%; negative cases: 66%). NF, nuclear factor; EGF, epidermal growth factor.

evaluated pretreatment specimens, recurrent tumors from 29 (83%) patients could be evaluated and compared with their pretreatment tumors, whereas those of the 6 patients who had been diagnosed at other hospitals could not. Twenty-six of 29 (90%) recurrent tumors showed positive NF-κB expression, compared with only 62 of 105 (60%) pretreatment tumors ($p = .004$) (Table 4).

Sixteen of 22 patients (73%) with pretreatment tumors that were NF-κB positive showed enhanced expression in recurrent tumors, whereas all patients with pretreatment tumors negative for NF-κB converted to NF-κB–positive recurrent tumors (see Figure 3). In total, NF-κB expression was dramatically enhanced in 23 of 29 (80%) recurrent tumors.

DISCUSSION

Early-stage laryngeal cancer constitutes a wide spectrum of disease, and treatment choices depend on factors such as tumor volume and extent; involvement of the anterior commissure; lymph node metastasis; patient age, occupation, preference, and compliance; availability of expertise in radiotherapy or surgery; and history of a malignant lesion in the head and neck.[9] There are no randomized studies comparing radiotherapy with conservation surgery regarding local control or survival for patients with early-stage laryngeal cancer. Similarly, there are no randomized controlled data comparing functional outcomes, specifically voice quality or swallowing ability.[9] Therefore, biological markers to predict radioresistant tumors may be useful prognostic tools.

Several biological markers may predict the local controllability in early-stage laryngeal cancer, but the findings are often controversial. For example, bcl-2 has been proposed,[14,26] but also argued against,[27,28] and EGF has also been proposed[15] and shown not to be an effective prognostic marker.[28,29] Many have also argued that the status of p53 is not an appropriate marker for prognosis or clinical outcomes.[13,16,28] We found that NF-κB expression showed the strongest correlation with local tumor control relative to bcl-2 or EGF receptor expression. In our study, nuclear NF-κB expression was also evaluated separately, but it was difficult to determine whether NF-κB was more tightly associated with local recurrence. It was speculated that this result might be explained by the difficulty of evaluation of nuclear expression. As for reduction of positive tumors when nuclear NF-κB expression was used, several investigators have reported similar

Table 3. Analyses of prognostic factors for local tumor control.

Variable	Tests for favorable status	HR	95% CI	*p* value
Univariate analyses				
NF-κB expression	Positive ($n = 62$) vs negative ($n = 43$)			.008
Age, y	≤60 ($n = 18$) vs >60 ($n = 87$)			.98
Sex	Male ($n = 97$) vs female ($n = 8$)			.93
Brinkman Index*	≤600 ($n = 19$) vs >600 ($n = 71$)			.76
Tumor location	Glottic ($n = 88$) vs nonglottic ($n = 17$)			.02
Tumor classification	T1 ($n = 67$) vs T2 ($n = 38$)			.03
Radiation dose, Gy	≤66 ($n = 57$) vs >66 ($n = 48$)			.07
OTT, days	≤45 ($n = 41$) vs >45 ($n = 64$)			.30
Bcl-2 expression	Positive ($n = 93$) vs negative ($n = 12$)			.85
EGF receptor expression	Positive ($n = 78$) vs negative ($n = 27$)			.55
Multivariate analyses				
NF-κB expression	Positive ($n = 62$) vs negative ($n = 43$)	0.43	0.18–0.99	.04
Tumor location	Glottic ($n = 88$) vs nonglottic ($n = 17$)	0.53	0.24–1.13	.10
Tumor classification	T1 ($n = 67$) vs T2 ($n = 38$)	0.75	0.37–1.56	.43

Abbreviations: NF-κB, nuclear factor-kappa B; EGF receptor, epidermal growth factor receptor; OTT, overall treatment time; HR, hazard ratio; CI, confidence interval.
**In all, 90 patients were available to be analyzed.*

results in other malignancies. Ross and colleagues[25] analyzed NF-κB expression in prostate adenocarcinomas and reported that 66 of 136 (49%) prostate adenocarcinomas expressed cytoplasmic NF-κB and that 20 of 136 (15%) expressed nuclear NF-κB. Sasaki et al[30] also analyzed NF-κB expression in gastric carcinomas and reported that the mean percentages of cytoplasmic and nuclear expression of NF-κB in tumor cells were 70.4% and 22.5%, respectively. Our results seemed to be consistent with these reports.

Although NF-κB expression significantly correlated with local control, the PPV for NF-κB expression was slightly low, at 0.44. We assessed whether any combination with other biological markers might improve this PPV. The PPVs of NF-κB and bcl-2, NF-κB, and EGF receptor and a combination of NF-κB, bcl-2, and EGF receptor were 0.42, 0.4, and 0.39, respectively (Table 2). Therefore, at least in our series, no combination showed stronger abilities compared with the single marker of NF-κB as for PPV. Using nuclear NF-κB expression also did not remarkably improve PPV. Larger scales of prospective studies will be required to conclude whether a single marker of the NF-κB or any combination with other biological markers might be a more powerful predictor for radioresistant tumors in the future.

Our results also indicate that NF-κB expression may be an independent prognostic factor in early-stage laryngeal cancer. Tumor classification, total dose, and OTT are common prognostic factors for local tumor control.[31–33] In this study, a case-control design matching those factors was performed to minimize their influence, but both tumor location, which was imbalanced because of the smaller number of patients with nonglottic disease, and tumor classification reached prognostic significance in univariate analysis. Therefore, to confirm the prognostic value of NF-κB expression, larger and more prospective studies are also warranted.

Another important finding in this study is the enhanced NF-κB expression in recurrent laryngeal cancers. NF-κB is activated by ionizing radiation in cancer cells.[34,35] Fan et al[36] reported that exposure to low-dose ionizing radiation induced adaptive radioresistance in mouth skin epithelial cells and activation of NF-κB, whereas inhibition of NF-κB blocked this radioresistance. Ahmed and Li[37] showed that activation of NF-κB was required for adaptive radioresistance and might mediate tumor radioresistance. Therefore, our results are consistent with those

Table 4. Comparison of NF-κB expression between pretreatment and recurrent tumors.

	NF-κB expression		
	Positive	Negative	*p* value
Pretreatment tumors ($n = 105$)	62	43	.004
Recurrent tumors* ($n = 29$)	26	3	

Abbreviation: NF-κB, nuclear factor-kappa B.
**In all, 29 of 35 recurrent tumors were available.*

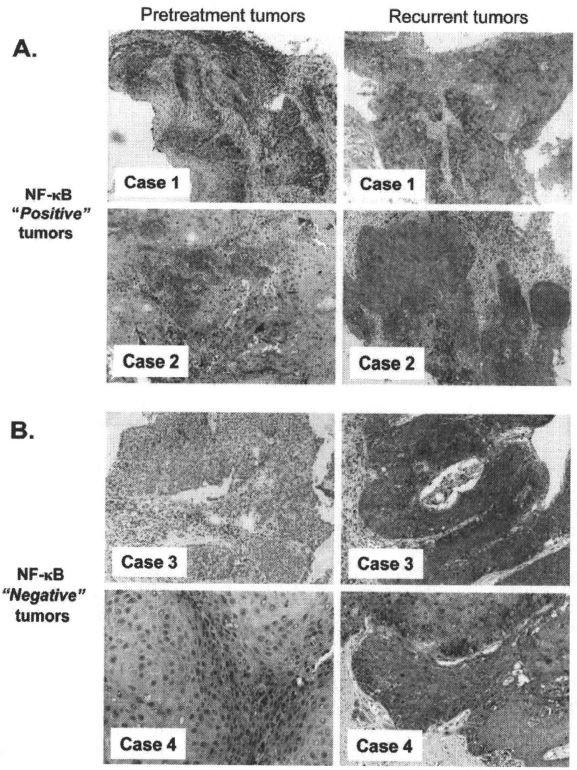

FIGURE 3. Comparison of NF-κB expression between pretreatment (left panels) and recurrent (right panels) tumors in 4 patients with early-stage laryngeal cancers. (**A**) NF-κB "*positive*" cases: case 1 (65 years old, male, T2 supraglottic) and case 2 (59 years old, male, T1a glottic). (**B**) NF-κB "*negative*" cases: case 3 (60 years old, female, T1a glottic) and case 4 (63 years old, male, T1a glottic). NF, nuclear factor.

experiments. However, several specimen-related factors could affect the enhancement of NF-κB expression in recurrent tumors. One of these factors is the condition of specimen storage. At our institution, all paraffin-embedded specimens were stored under the correct temperature and humidity conditions. The shorter storage times for recurrent tumors could also affect the result, but in fact, the specimen storage times were not different: pretreatment tumors were stored for 93 months (range, 28–215) after histological evaluation, and recurrent tumors were stored for 86 months (range, 19–185) ($p = .26$ by a t test), suggesting that storage time did not influence these results. Patient-related factors, such as smoking, chemotherapy, and infection, could also enhance NF-κB expression. We believe that the enhancement was mainly attributable to radioresistance, but further examination with extreme caution is required to exclude the influence of these factors.

Benefits of using such predictive radioresistant markers in the treatment of early-stage laryngeal cancer are to provide further improvements in treatment outcomes, including laryngeal preservation rate. Prediction of radioresistant tumors may allow us to choose more aggressive strategies such as concurrent chemoradiotherapy or to choose laryngeal preserving surgery combined with radiotherapy in such cases instead of radiotherapy alone. Therefore, prospective studies for the use of predictive markers including NF-κB should be performed. Moreover, a novel strategy targeting inhibition of NF-κB against radioresistant laryngeal cancer should also be proposed. In the clinical field, few studies demonstrate that targeting NF-κB might achieve improvement in treatment outcomes. Van Waes and colleagues[38] reported the results of their study targeting inhibition of NF-κB using a proteasome inhibitor in patients with recurrent head and neck squamous cell carcinoma. In that study, some cases showed effective responses, whereas others progressed. Thus, effectiveness of the inhibition of NF-κB has not yet been proven. Several investigators have reported that activation of NF-κB is an important step for protection from radiation-induced damage in normal tissue.[39–41] Therefore, when a novel radiotherapeutic strategy combined with inhibition of NF-κB is proposed, attention must be paid to the possibility that the combination may increase not only the toxicity of the radiotherapy, but also its efficacy. Our results also involve the possibility that targeting NF-κB combined with radiotherapy may be a useful tool for radioresistant tumors, but many problems must be overcome.

In conclusion, this report includes 2 important findings. First, NF-κB expression was correlated with local tumor control and was a strong prognostic factor in early-stage laryngeal cancer. Second, NF-κB expression was dramatically enhanced in recurrent laryngeal cancer. Thus, NF-κB may play an important role in the radioresistant mechanisms of early-stage laryngeal cancer.

REFERENCES

1. Vokes EE, Weichselbaum RR, Lippman SM, Hong WK. Head and neck cancer. N Engl J Med 1993;328:184–194.
2. Shaha AR, Shah JP. Carcinoma of the subglottic larynx. Am J Surg 1982;144:456–458.
3. Mendenhall WM, Mancuso AA, Hinerman RW, et al. Multidisciplinary management of laryngeal carcinoma. Int J Radiat Oncol Biol Phys 2007;69:S12–S14.
4. Mendenhall WM, Werning JW, Hinerman RW, Amdur RJ, Villaret DB. Management of T1–T2 glottic carcinomas. Cancer 2004;100:1786–1792.
5. Ton-Van J, Lefebvre JL, Stern JC, Buisset E, Coche-Dequeant B, Vankemmel B. Comparison of surgery and radiotherapy in T1 and T2 glottic carcinomas. Am J Surg 1991;162:337–340.
6. Benninger MS, Gillen J, Thieme P, Jacobson B, Dragovich J. Factors associated with recurrence and voice quality following radiation therapy for T1 and T2 glottic carcinomas. Laryngoscope 1994;104:294–298.
7. Krengli M, Policarpo M, Manfredda I, et al. Voice quality after treatment for T1a glottic carcinoma—radiotherapy versus laser cordectomy. Acta Oncol 2004; 43:284–289.
8. McGuirt WF, Blalock D, Koufman JA, et al. Comparative voice results after laser resection or irradiation of T1 vocal cord carcinoma. Arch Otolaryngol Head Neck Surg 1994;120:951–955.
9. Pfister DG, Laurie SA, Weinstein GS, et al. American Society of Clinical Oncology clinical practice guideline for the use of larynx-preservation strategies in the treatment of laryngeal cancer. J Clin Oncol 2006;24:3693–3704.
10. McLaughlin MP, Parsons JT, Fein DA, et al. Salvage surgery after radiotherapy failure in T1–T2 squamous cell carcinoma of the glottic larynx. Head Neck 1996; 18:229–235.
11. Burke LS, Greven KM, McGuirt WT, Case D, Hoen HM, Raben M. Definitive radiotherapy for early glottic carcinoma: prognostic factors and implications for treatment. Int J Radiat Oncol Biol Phys 1997;38:1001–1006.
12. Small W Jr, Mittal BB, Brand WN, et al. Results of radiation therapy in early glottic carcinoma: multivariate analysis of prognostic and radiation therapy variables. Radiology 1992;183:789–794.
13. Pai HH, Rochon L, Clark B, Black M, Shenouda G. Overexpression of p53 protein does not predict local-regional control or survival in patients with early-stage squamous cell carcinoma of the glottic larynx treated with radiotherapy. Int J Radiat Oncol Biol Phys 1998; 41:37–42.
14. Nix P, Cawkwell L, Patmore H, Greenman J, Stafford N. Bcl-2 expression predicts radiotherapy failure in laryngeal cancer. Br J Cancer 2005;92:2185–2189.
15. Demiral AN, Sarioglu S, Birlik B, Sen M, Kinay M. Prognostic significance of EGF receptor expression in early glottic cancer. Auris Nasus Larynx 2004;31:417–424.
16. Parikh RR, Yang Q, Haffty BG. Prognostic significance of vascular endothelial growth factor protein levels in T1–2 N0 laryngeal cancer treated with primary radiation therapy. Cancer 2007;109:566–573.
17. Nix PA, Greenman J, Cawkwell L, Stafford N. Radioresistant laryngeal cancer: beyond the TNM stage. Clin Otolaryngol Allied Sci 2004;29:105–114.
18. Aggarwal BB. Nuclear factor-κB: the enemy within. Cancer Cell 2004;6:203–208.
19. Karin M, Ben-Neriah Y. Phosphorylation meets ubiquitination: the control of NF-κB activity. Ann Rev Immunol 2000;18:621–663.
20. Baldwin AS Jr. The NF-κB and IκB proteins: new discoveries and insights. Annu Rev Immunol 1996;14:649–683.
21. Karin M, Cao Y, Greten FR, Li ZW. NF-κB in cancer: from innocent bystander to major culprit. Nat Rev Cancer 2002;2:301–310.

22. Ghosh S, May MJ, Kopp EB. NF-κB and Rel proteins: evolutionarily conserved mediators of immune responses. Ann Rev Immunol 1998;16:225–260.
23. Izzo JG, Malhotra U, Wu TT, et al. Association of activated transcription factor nuclear factor-κB with chemoradiation resistance and poor outcome in esophageal carcinoma. J Clin Oncol 2006;24:748–754.
24. Siebenlist U, Brown K, Claudio E. Control of lymphocyte development by nuclear factor-κB. Nat Rev Immunol 2005;6:435–445.
25. Ross JS, Kallakury BV, Sheehan CE, et al. Expression of nuclear factor-κB and IκB alpha proteins in prostatic adenocarcinomas: correlation of nuclear factor-κB immunoreactivity with disease recurrence. Clin Cancer Res 2004;10:2466–2472.
26. Condon LT, Ashman JN, Ell SR, Stafford ND, Greenman J, Cawkwell L. Overexpression of Bcl-2 in squamous cell carcinoma of the larynx: a marker of radioresistance. Int J Cancer 2002;100:472–475.
27. Ogawa T, Shiga K, Tateda M, et al. Protein expression of p53 and Bcl-2 has a strong correlation with radiation resistance of laryngeal squamous cell carcinoma but does not predict the radiation failure before treatment. Oncol Rep 2003;10:1461–1466.
28. Kamijo T, Yokose T, Hasebe T, et al. Potential role of microvessel density in predicting radiosensitivity of T1 and T2 stage laryngeal squamous cell carcinoma treated with radiotherapy. Clin Cancer Res 2000;6: 3159–3165.
29. Wen QH, Miwa T, Yoshizaki, T, Nagayama I, Furukawa M, Nishijima H. Prognostic value of EGFR and TGF-alpha in early laryngeal cancer treated with radiotherapy. Laryngoscope 1996;106:884–888.
30. Sasaki N, Morisaki T, Hashizume K, et al. Nuclear factor-κB p65 (RelA) transcription factor is constitutively activated in human gastric carcinoma tissue. Clin Cancer Res 2001;7:4136–4142.
31. Le QT, Fu KK, Kroll S, et al. Influence of fraction size, total dose, and overall time on local control of T1–T2 glottic carcinoma. Int J Radiat Oncol Biol Phys 1997;39: 115–126.
32. Rudoltz MS, Benammar A, Mohiuddin M. Prognostic factors for local control and survival in T1 squamous cell carcinoma of the glottis. Int J Radiat Oncol Biol Phys 1993;26:767–772.
33. Terhaard CH, Snippe K, Ravasz LA, van der Tweel I, Hordijk GJ. Radiotherapy in T1 laryngeal cancer: prognostic factors for locoregional control and survival, uni- and multivariate analysis. Int J Radiat Oncol Biol Phys 1991;21:1179–1186.
34. Brach MA, Hass R, Sherman ML, Gunji H, Weichselbaum R, Kufe D. Ionizing radiation induces expression and binding activity of the nuclear factor-κB. J Clin Invest 1991;88:691–695.
35. Voboril R, Weberova-Voborilova J. Sensitization of colorectal cancer cells to irradiation by IL-4 and IL-10 is associated with inhibition of NF-κB. Neoplasma 2007;54: 495–502.
36. Fan M, Ahmed KM, Coleman MC, Spitz DR, Li JJ. Nuclear factor-κB and manganese superoxide dismutase mediate adaptive radioresistance in low-dose irradiated mouse skin epithelial cells. Cancer Res 2007;67:3220–3228.
37. Ahmed KM, Li JJ. NF-κB-mediated adaptive resistance to ionizing radiation. Free Radic Biol Med 2008;44:1–13.
38. Van Waes C, Chang AA, Lebowitz PF, et al. Inhibition of nuclear factor-κB and target genes during combined therapy with proteasome inhibitor bortezomib and reirradiation in patients with recurrent head-and-neck squamous cell carcinoma. Int J Radiat Oncol Biol Phys 2005;63:1400–1412.
39. Wang Y, Meng A, Lang H, et al. Activation of nuclear factor κB In vivo selectively protects the murine small intestine against ionizing radiation-induced damage. Cancer Res 2004;64:6240–6246.
40. Egan LJ, Eckmann L, Greten FR, et al. IκB-kinase beta-dependent NF-κB activation provides radioprotection to the intestinal epithelium. Proc Natl Acad Sci U S A 2004;101:2452–2457.
41. Sonis ST. The biologic role for nuclear factor-κB in disease and its potential involvement in mucosal injury associated with anti-neoplastic therapy. Crit Rev Oral Biol Med 2002;13:380–389.

2．PET診断と放射線治療

神戸大学大学院医学研究科内科系講座放射線医学分野放射線腫瘍学部門　特命准教授　佐々木良平

1．はじめに

FDG-PET の登場と日常診療への定着により放射線治療の体系は大きく転換したと言える。欧米ではかねてから放射線腫瘍医が FDG-PET を積極的に診療の体系の中に組み入れてきたが、近年では本邦でも同様の傾向が見られ、広く日常臨床のがん診療の中に取り入れられつつある。言うまでもなく放射線治療はその根治的な方針、緩和的な方針に関わらず局所的な治療であり、治療対象となる病変の部位、広がり、個数は極めて重要であるが、FDG-PET から得られる情報によって治療方法が変更されることも多々ある。その中でも本号では放射線腫瘍医の視点から、頭頸部がん、乳がん、悪性リンパ腫、原発不明がん、肺がん、食道がん等の FDG-PET が特に有用とされる疾患において、放射線治療の依頼を受けた時点から治療計画、効果判定、更には治療後の経過観察時において、FDG-PET をどの様に活用すれば、誤ることなく更に有効に活用できるかに焦点を絞って概説し、後半では FDG-PET の半定量法の一つである Standardized Uptake Value (SUV)を用いた非小細胞肺癌における予後予測に関しての自著の報告[1]から要約する。

2．放射線治療における FDG-PET の役割

FDG-PET の有用性は多岐にわたり様々な場面で活用されているが、大別すると(1) Initial Staging（初回治療時の病期決定）、(2) Restaging(再発時の病変の広がり診断)、(3) Response Evaluation（治療効果判定）、(4) Delineating Tumor Targets（放射線治療の標的部位の輪郭を囲む）、(5) Predict Outcome（予後予測）となる。したがって FDG-PET 検査を依頼する側の医師は、検査の目的は何であるかを適切に検査側に伝え、FDG-PET 検査の所見レポートを作成する医師も、依頼者の目的は何かを確認して適切な情報を導き出してレポートを作成する努力が望まれる。(6) として、胸部放射線治療後の放射線肺線維症内の再発腫瘍の判定に関する意義に関して注意すべき課題を述べる。

2．1 Initial Staging

FDG-PET は非小細胞肺がん、食道がん、悪性リンパ腫、頭頸部がん、原発不明がん等の疾患で初回治療時の病期決定に特に有用であるが、その一方で肺胞上皮がんや、MALT Lymphoma 等では FDG の集積が弱い症例が多く、病期決定の際にもその腫瘍の特性に特に注意が必要である。更にリンパ節転移の有無に関しては CT に加えて PET を施行することによりその正診率が向上し、Baardwijk 等は[2]、肺がんの領域リンパ節診断においては Sensitivity が 71～91% (PET with CT) vs. 22～83% (CT); Specificity が 67～92% (PET with CT) vs. 66～90% (CT); Accuracy が 73～92% vs. 65～80%と報告している。

食道がんのリンパ節診断においても、Sensitivity が 5～74% (PET with CT) vs. 47～50% (CT); Specificity が 84～90% (PET with CT) vs. 69% (CT); Accuracy が 82～83%(PET with CT) vs. 64～68%(CT)とその有効性が報告されている。放射線治療分野においても、大西ら[3]を中心に本邦から世界的に発展した I 期非小細胞がんに対する体幹部定位的放射線治療においても、FDG-PET を用いてリンパ節転移や遠隔転移が存在しないことを確認することは極めて重要である。また、図１は原発不明がんとして頸部リンパ節に対する放射線治療を依頼された症例である。紹介元の病院ではルーチンの咽頭・喉頭観察と CT、MRI の画像検査にて原発巣を確定できなかったが、FDG-PET を実施することで下咽頭に潜在していた微小な腫瘍を発見でき、放射線治療に関する治療方針が変更になった症例である。近年では多くの施設で原発不明がんに対して FDG-PET は必須の検査として実施されているが、本症例のように特に放射線治療の方法（部位、処方線量）に関しても極めて重要な情報となることを留意したい。

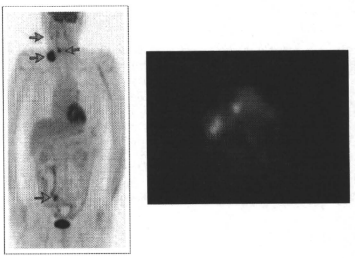

図１　62 歳、男性。原発不明頸部リンパ節転移を有する症例であったが FDG-PET にて下咽頭癌および頸部リンパ節転移と確定された。

2．2 Restaging

肺がんや食道がんにおいては言うまでも無く、乳がんや悪性リンパ腫など多くの悪性腫瘍では、再発腫瘍が診断された時点で、それ以外の部位や他臓器にもさらなる病変が潜在している可能性を慎重に考慮することが放射線腫瘍医を含めた全てのがん治療医に求められる。同様にそのような場面で放射線治療医から FDG-PET 検査を依頼された場合には、その依頼医師の主旨を十分に理解した診断レポートを作成することが要求される。繰り返すが放射線治療は局所治療なので、FDG-PET を用いた全身の精査にて病変の部位、広がりを把握する意義は極めて大きい。初回治療時の病期にもよるが、筆者らは肺がんや食道がん、乳がんなどの症例では、再発腫瘍に対する放射線治療を依頼された場合には、できる限り FDG-PET での全身検索と脳の造影 MRI を組み合わせて Restaging を実施している。特に乳がん症例で局所や鎖骨上窩に再発腫瘍やリンパ節腫脹が診断された場合には、患側の胸壁や鎖骨上窩に対しての定型的な術後照射の依頼を受けるが、このような場合でも FDG-PET は極めて有用な他部位病変に関する情報を提供することが多い。実際に図２の如く、胸腹部の CT 検査にて遠隔転移がな

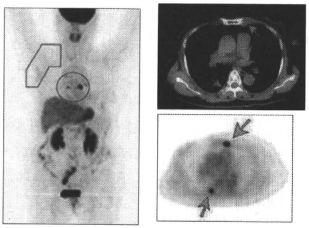

図２　70歳、女性。乳がんの乳房切断術後。
患側の鎖骨上窩～腋窩（赤線）に対する放射線治療を依頼されたが、FDG-PETにより多発骨転移（青曲線、矢印）が指摘され治療方針の変更となる。

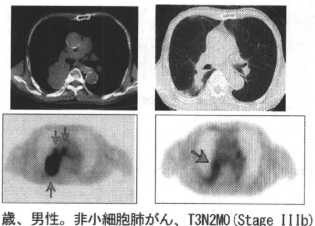

図３　76歳、男性。非小細胞肺がん、T3N2M0（Stage IIIb）の症例。
左上：治療前CT、左下：治療前FDG-PET、右上：治療後６ヵ月時点のCT、左下：治療後６ヵ月時点のFDG-PET。治療後６ヵ月の時点ではCTではPRの診断であるが、FDG-PETではbiological CRと診断され、治療後経過５年でもCRを持続している。

いという診断の元に領域リンパ節領域である患側の鎖骨上窩の術後照射を依頼された症例においてFDG-PETを実施すると、既に遠隔転移を指摘され、治療方針が変更になった症例を経験する事は多い。FDG-PETを施行しなければ既存の病変が無治療のまま放置し、実際に臨床上問題とならない部位に対して予防照射を実施するという事にもなりかねない。このような場合、依頼された細胞レベルでの腫瘍残存を想定した鎖骨上窩の術後照射の意義は極めて乏しいため、FDG-PETによる診断で得られた正確な情報を患者に伝え、治療方法を変更することとなる。このように、FDG-PETを軸にした正確な病状把握を元にして、最適の治療の選択肢の提示をしていく姿勢は、これからの臨床の現場でも益々増えていくことと予想される。

2．3 Response evaluation

近年、放射線治療や放射線化学療法に対してのFDG-PETを用いた治療効果判定に関しても有用な報告が多数認められる[4-7]。FDG-PETは機能画像であり、CTやMRIなどの形態画像による治療効果判定とは、根本的にその意味する内容、意義が異なる。特に腫瘍径の大きな腫瘍では放射線治療や放射線化学療法後に、腫瘍の最大径は大きく変化せずとも著明な抗腫瘍効果が認められ、後々の経過観察においても腫瘍の再燃を見ないこともある。図３に自験例を示すがCTではあまり縮小を認めず、PRやNCの範疇の治療効果であってもFDG-PETではほぼ完治していることを反映する結果（biological CR）が得られ、その後の経過観察でも再発を認めず、FDG-PETの結果が病態をより適確に反映していることも度々経験される。また、一方で非小細胞がんの症例において根治的な放射線治療後６ヵ月を経過しても腫瘍に対して集積が低下せず、数年後に集積が低下した症例も稀ではあるが経験される。このようにFDG-PETを用いた治療効果の判定に関しては、更なるデータの集積が必要と思われ、特にそれぞれの疾患に適したFDG-PET施行のタイミングを検討することが重要と思われる。

このように従来、診断が困難であった場面でもFDG-PETを活用すれば、数年の経過観察の期間を待たずとも迅速に診断可能なことが多い。ただし、現時点では、放射線肺臓炎、亜急性期の放射線肺繊維症に関しては FDG の集積に程度に関してまとまった報告は認められず、診断の根拠になりうる報告がない。その意味でもFDG-PETを効果判定に用いる時期に関しては今後更なる検討が必要であると考えられる。

2．4 Delineating Tumor Targets

放射線治療計画では、腫瘍の輪郭を囲み（Contouring）腫瘍体積（Gross Target Volume = GTV、Clinical Target Volume = CTV）、そして由来臓器・隣接臓器（Organs at Risk）の被照射体積との考案の中で、最適の照射法を検討する作業が中心となる。この治療計画は通常 3～5mm 間隔 CT 水平断を用いて行われるが、原発腫瘍に関しても領域リンパ節に関してもその計画者同士における輪郭の囲み方の差異が問題となる。そのAccuracy に関しては Initial staging に前述したのでここでは詳細は省略するが、特に肺門肺がんでその末梢に無気肺を呈した場合などで FDG-PET が特に有用である。CT のみでは CTV の設定が困難であるが、FDG-PET を用いることにより、腫瘍の範囲をより正確に示すことが可能である（図４）。つまり治療計画において FDG-PET の情報を治療計画の現場においても積極的に活用していくことが必要であり、詳細に関しては諸家の報告を参考にされたい[8-10]。

2．5 Predict Outcomes

非小細胞肺がんにおける FDG-PET の SUV を用いた予後予測に関して概説する。日常診療や諸家の報告からは、非小細胞がんでは従来の大きさを元にした病期（TNM）分類だけでは、たとえ早期がんでも転移や再発を多々経験するため、形態による病期分類だけではそれぞれの疾患の予後を予測することは必ずしも容易ではなく、腫瘍の悪性度や転移能などの機能を反映した病期分類が期待されている。我々は米国 MD Anderson Cancer Center で根治的治療を施行された 162 例に関して（手術群 93 例、放射線治療群 69 例）、その治療前の FDG-PET の結果を遡及的に解析した。

それらの検討症例での解析では原発腫瘍の SUV のカットオフ値は“５”が全体生存率、腫瘍制御率ともに最も有用な値であったので、それを用いて検討したところ、図５に示すように手術群、放射線治療群共に原発腫瘍の SUV 値が統計学的に有意な腫瘍制御因子であることが確認され、また一方で図６の如く同じ病期（stage I/II, vs.Stage III）であっても SUV 値によって腫瘍制御率が極めて異なることを報告した。更に数々の予後因子を単変量解析で個別に
解析し、その結果を比較した中でも原発腫瘍の SUV は最も有益な予後因子であった（表１）。詳細に関しては紙面の都合上、文献１を参照されたい。

2．6 放射線肺線維症内部の照射野内再発の診断における FDG-PET の有用性

原発性、転移性肺腫瘍に対して放射線治療を施行後、CT では放射線肺線維症の内部における局所再発腫瘍を早期に診断することは困難な場合が多い。FDG-PET は再発腫瘍の診断に有用である可能性を有するが、その診

表 1　非小細胞肺がんにおける局所制御に関与する因子の解析。
原発腫瘍の SUV 値は他の因子と比較しても最も強い意味を持つ因子である。

Factors		Relative risk	P value
SUV for primary tumor	(≦5.0 vs. >5.0)	5.09	<0.0001
Treatment	(Surgery vs. Radiotherapy)	0.81	0.405
T stage	(T1, T2 vs. T3, T4)	2.97	<0.0001
N stage	(N0, N1 vs. N2, N3)	1.77	0.025
Clinical stage	(Stage Ⅰ/Ⅱ vs. stage ⅢA/B)	2.18	0.002
Tumor size	(<4.0cm vs. ≧4.1cm)	1.20	0.001
Histology	(Squamous vs. non-squamous)	0.76	0.264
Age	(<60 vs. ≧60)	0.97	0.922
Gender	(Male vs. Female)	1.20	0.270
KPS	(<80 vs. ≧80)	0.58	0.031
Weight loss	(<5% vs. ≧5%)	1.16	0.617
SUV for LNs	(≦5.0 vs. >5.0)	0.60	0.049

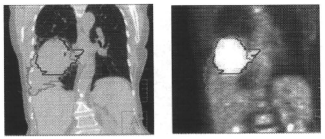

図 4　73 歳、男性。非小細胞肺がんの症例。
CT のみでは腫瘍部（赤線）と無気肺の正常部との境界が不明であり、CTV は双方を含めて（緑線）設定せざるを得ないが、FDG-PET を併用することにより CTV を腫瘍部に限局して正確に設定できる。

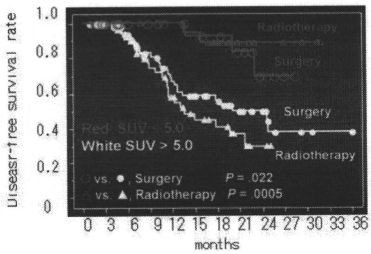

図 5　FDG-PET を用いた非小細胞癌における治療法別の検討。
手術（Surgery）群（n=93）と放射線治療（Radiotherapy）群（n=69）双方における腫瘍制御率を SUV 値（cut-off, 5.0）を用いて比較。手術群、放射線治療群、いずれにおいても SUV が 5 以下の群で良好な腫瘍制御率を示す。（文献 1 より引用）

断にはまず根治的な放射線治療を施行した際の放射線肺障害の経過と病理学的な成り立ちを理解し、FDG-PET の実施時期に応じてどのような病理学的な背景を反映しているかを理解する必要がある。具体的には放射線治療後 3 ヵ月以内では被照射部位では肺胞を構成する種々の細胞によるサイトカインの分泌が活発であり、そこに炎症細胞浸潤が加わるとされる。FDG-PET ではそれらの組織修復過程を反映するためか、腫瘍の再発がなくとも照射体積全体に集積が強いことが一般的である。つまりこの時期に FDG-PET 検査を実施しても再発腫瘍の判定は困難であると考えられる。放射線治療後 6 ヵ月以降は放射線治療に起因する肺の線維化がほぼ完成するため、FDG-PET 検査で集積が認められた場合には局所再発を意味することが多い。しかし、照射部位に FDG の集積が認められた場合にも部分的な感染症などによる疑陽性の

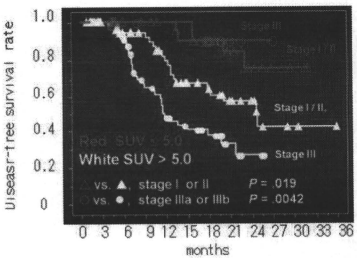

図 6　FDG-PET を用いた非小細胞癌における病期別に検討。
早期群（Stage Ⅰ/Ⅱ, n=90）と進行群（Stage Ⅲ, n=72）での SUV 値（cut-off, 5.0）を用いて比較。早期群、進行群いずれにおいても SUV が 5 以下の群で良好な腫瘍制御率を示す。（文献 1 より引用）

場合もあり、臨床的な診断と放射線治療後の経過を慎重に加味して判断していくことが肝要である。

3．おわりに

FDG-PET は今日のがん診療の中で単に悪性腫瘍を拾い上げて病期診断に用いるだけでなく、治療効果の判定や予後予測など放射線治療医だけでなく外科医や腫瘍内科医に対しても欠くべからざる有用な情報を提示することが可能であり、近年で日常臨床の中でしっかりその存在意義を認められたといっても過言ではない。さらに SUV 値は定性的な所見よりもさらに有用な情報をもたらすことが多いが、測定方法によって SUV 値の反映している　病態は異なり、施設間で端的に比較できるものではないことを今一度確認しておく必要がある。それでも FDG-PET は放射線腫瘍学の発展とともにその活用方法はさらに 拡大していくことが予想される。

4．文献

1) Sasaki R, et al. J Clin Oncol. 23(6):1136-43, 2005.
2) van Baardwijk A, et al.Cancer Treat Rev. 32(4):245-60, 2006.
3) Onishi H, et al. Cancer. 101(7):1623-31, 2004.
4) Ryu JS, et al. Lung Cancer.35:179-187, 2002.
5) Hoekstra CJ, et al. Lung Cancer 39:151-157, 2003.
6) MacManus MP, et al. J Clin Oncol 21:1285-1292, 2003.
7) Song SY, et al. Int J Radiat Oncol Biol Phys. 63(4):1053-9, 2005.
8) Greco C, et al. Lung Cancer. 2007 May 1; [Epub ahead of print]
9) van Baardwijk A, et al. Cancer Treat Rev. 32(4):245-60, 2006.
10) Leong T, et al. Radiother Oncol. 78(3):254-61, 2006

DOI: 10.1021/cg900941p

CRYSTAL GROWTH & DESIGN
Communication
2010, Vol. 10
11–15

Preparation of Ba-Hexaferrite Nanocrystals by an Organic Ligand-Assisted Supercritical Water Process

Dinesh Rangappa,*[,†,§] Takashi Naka,[†] Satoshi Ohara,[§] and Tadafumi Adschiri*[,§]

[†]*Innovative Materials Engineering Laboratory, National Institute for Materials Science, Sengen 1-2-1, Tsukuba, Ibaraki 305-0047, Japan and* [§]*World Premier Research Institute-Advanced Institute of Materials Research, Tohoku University Katahira 2-1-1, Aoba-ku, Sendai 980-8579, Japan.* [⊥]*Currently working at Energy Technology Research Institute National Institute of Advanced Industrial Science and Technology (AIST) Umezono, 1-1-1, Tsukuba, Ibaraki 305-0012, Japan.*

Received August 9, 2009; Revised Manuscript Received November 11, 2009

ABSTRACT: We are reporting a novel synthetic approach to prepare organic modified Ba-hexaferrite nanocrystals with controlled size and morphology under a supercritical water (SCW) flow reactor process. The surface of the Ba-hexaferrite nanocrystal was capped with oleic acid ligand to control the particle growth, size, and morphology. The results showed that the concentration of oleic acid reagent played a key role in controlling the cubic and octahedral shape of Ba-hexaferrite nanocrystals. This indicates that the size and morphology of nanocrystals were greatly influenced by the organic modification under the SCW process, resulting in a drastic reduction in the particle size from 30 to 9 nm. The organic ligand capped Ba-hexaferrite nanocrystals exhibit a higher coercivity (about 2800 Oe) at 5 and 280 K temperature. This study provides a novel approach for large-scale production of complex metal oxide colloidal nanocrystals with uniform size, well-defined shape, and controlled surface chemistry.

Barium hexaferrite nanocrystals are scientifically and technologically very important material. It has been intensively investigated as a high-density media for perpendicular and longitudinal recording, because of its high saturation magnetization, good chemical stability, and large magnetocrystalline anisotropy, as well as for its mechanical hardness.[1] In nano composite form, it can be used for the absorption of microwave radiation, where the ferrimagnetic nanopowders exhibit a higher absorption at low field strength and a broader absorption range in the microwave region than multidomain powders.[2] For ideal performance in high density magnetic recording, $BaFe_{12}O_{19}$ nanocrystals with a particle size of less than 20 nm and high coercivity are required. A special synthetic approach is required to fulfill this requirement.[3] Various synthetic methods have been proposed to produce Ba-hexaferrite nanoparticles: microemulsion, chemical coprecipitation, glass crystallization, combustion, sol−gel synthesis, and hydrothermal synthesis.[4] Hakuta et al. developed a supercritical water method for the rapid production of Ba-hexaferrite.[5] However, it is difficult to obtain size- and shape-controlled Ba-hexaferrite nanocrystals, due to the lack of a suitable synthetic process.

Colloidal science obviously offers versatile routes for the control of bulk composition, size, shape, and the surface properties of nanoparticles.[6,7] Organic molecules, inorganic precursors, polymers, copolymers, and surface active agents are involved in the preparation of colloidal nanoparticles and their assembly into complex ordered architectures. By combining this concept and the properties of supercritical water (SCW),[8] our group and others have been successful in synthesizing the different metal oxide and hydroxide nanocrystals in a batch type reactor.[9,10] Using organic ligand molecules that are miscible with SCW, crystal growth can be limited and agglomeration can be inhibited in favor of small, well-dispersed particles.[11]

In this paper, we are reporting a facile method for the production of size- and shape-controlled Ba-hexaferrite nanocrystals capped with the oleic acid ligand by SCW flow reactor.

Experimental Procedures. The feed solution used in the flow reactor experiments was prepared by dissolving iron(III) nitrate ($Fe(NO_3)_3 \cdot 9H_2O$) and barium hydroxide ($Ba(OH)_2 \cdot 8H_2O$) in distilled water. The required amount of KOH (Wako Chemicals Ltd. Osaka, Japan) was added to get $BaFe(OH)_5$ precursor. The final concentration of this precursor solution was adjusted to 0.05 M with a Ba/Fe molar ratio of 0.5. On the other hand, 0.25−0.5 M modifier reagent solution was prepared by dissolving oleic acid in ethanol (Aldrich Chemicals). Double distilled water distilled by EYELA STILL ACE SA-2100E was used for all the preparations.

Sample Preparation by SCW Flow Reactor. The flow type tube reactor was used to prepare the Ba-hexaferrite samples. The schematic diagram of the flow type reactor is displayed in Figure 1. The tube reactor was made up of pressure-resistant SUS316 stainless steel and was 60 cm in length and 0.84 cm inner diameter with a volume of 33.4 cm^3. The reactor was maintained at a constant temperature by using an external heater. Temperature was measured at the reactor inlet, in the middle of the reactor, and at the reactor outlet, and then it was confirmed that the temperature distribution was uniform to within ±1 °C. The residence time, τ, calculated was 20 s. For synthesis of Ba-hexaferrite nanocrystals, high temperature water was fed through one line at the flow rate of 30 cm^3/min. A precursor solution of 0.05 mol/L concentration was fed from a second line at the flow rate of 6 mL/min and mixed with the high temperature water at mixing point MP1. The organic modifier solution was fed through a third line which mixes with high temperature water and precursor solution at mixing point MP2. The product was quenched to room temperature using a cold water cooling system and collected at the outlet. The reaction temperature was 450−500 °C with a pressure of 30 MPa at MP1 and about 350−380 °C at MP2. The collected product was washed with ethanol and centrifuged to collect the nanocrystals. The surface-modified particles are extracted with toluene.

Analytical Characterization. The XRD patterns were recorded on a RINT-2000 spectrometer (Rigaku, Tokyo, Japan) with Cu Kα radiation at 36 kV and 20 mA, at the scan rate of 2°/min, from 10 to 60 ° 2θ. The samples were ground to fine powders before being subjected to X-ray diffraction (XRD). The

*To whom correspondence should be addressed. E-mail: dineshrangappa@gmail.com (D.R.); ajiri@tagen.tohoku.ac.jp (T.A.).

Published on Web 11/20/2009

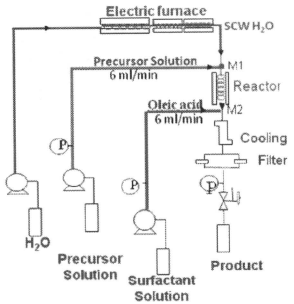

Figure 1. Schematic representation of the supercritical water flow type apparatus.

transmission electron microscopy (TEM) images were obtained using a TEM (JEM-1200EX, Japan) operated at 120 kV. Dynamic light scattering (DLS) measurements were done using Zetasizer Nano Series ((Nano ZS), Malvern Instruments, UK). The magnetic property was measured by a commercial superconducting quantum interference device magnetometer (SQUID) (MPMS XL7, Quantum design, USA). The powder sample was cast by a glue to avoid the reorientation of the individual crystals along the applied magnetic field.

Results and Discussion. The size- and shape-controlled Ba-hexaferrite nanocrystals were obtained by an organic ligand assisted SCW method using a flow type reactor. As-prepared nanocrystals can be dispersed well in toluene and they remain stable for several months. The average particle size of the organic modified Ba-hexaferrite nanocrystals was measured by DLS. The measured DLS particle size is about 11 nm, and the histogram of the particle size distribution is shown in Figure 2. This DLS size includes the size of the oleic acid ligand and the solvent ion. The DLS size excluding the organic ligand is more or less comparable to the particle size obtained from TEM and XRD data. The DLS measurement revealed that the majority of nanoparticles were nonagglomerated, resulting with stable Ba-hexaferrite nanocrystals in a nonpolar solvent. Such stable suspensions of ferrofluids can be used in many technological applications.

Crystallographic Analysis. The XRD patterns of the Ba-hexaferrite samples prepared with a Ba:Fe molar ratio of 0.5 at temperature 450−500 °C and 30 MPa indicated that the nanocrystals formed under SCW conditions exhibit a primitive hexagonal structure (Figure 3) with space group, $P6_3/mmc$ (194) that match well with the JCPDS card (PDF #39-1433). The effects of Ba/Fe mole ratios on the phase composition of products have been reported by several researchers.[4] It can be observed that the nonstoichiometric ratio resulted in single phase Ba-hexaferrite particles. Most of the reports indicate that an increase in the Ba concentration promoted the formation of Ba-hexaferrite phase with the different synthetic procedure. In this study, we have observed that the Ba-hexaferrite single phase was formed at a Ba/Fe mole ratio of 0.5. The stoichiometric mole ratio of Ba/Fe resulted in α-Fe_2O_3 as an impurity phase along with Ba-hexaferrite. Hakuta et al. reported the effect of Ba/Fe molar ratios on Ba-hexaferrite formation under similar supercritical water conditions using both flow and batch type reactors in the absence of organic molecules. The results obtained in this study are consistent with the results reported by Hakuta et al. The XRD patterns of the Ba-hexaferrite

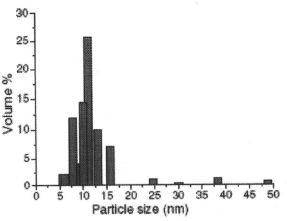

Figure 2. Particle size distribution of the Ba-hexaferrite colloidal nanocrystals capped with oleic acid ligand dispersed in toluene measured by DLS.

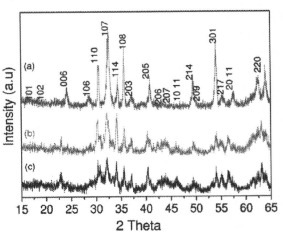

Figure 3. Powder X-ray diffraction patterns of the Ba-hexaferrite nanocrystals; (a) with uncapped surface, (b) and (c) capped with oleic acid ligand under supercritical water conditions at 400 °C temperature and 30 MPa pressure.

nanocrystal synthesized in the absence and presence of the organic ligand molecules are shown in Figure 3. When the organic ligand molecules were introduced into the reaction system, the organic ligand absorbed onto the surface of nanocrystal and capped the surface to restrict the growth of the nanoparticles. The XRD patterns of the nanocrystal capped with oleic acid molecules indicate that the intensity of peaks decreased with a small peak broadening. This suggests that the size of the nanocrystals were decreased with organic modification. The average crystallite size of the Ba-hexaferrite nanocrystals synthesized in the absence and presence of the organic ligand was calculated by the XRD data using Scherrer's law. The average crystallite sizes of bare and organic modified Ba-hexaferrite nanocrystals are 30 and 8.5 nm, respectively.

Size and Morphology. The size and morphology of the Ba-hexaferrite nanocrystals prepared by the SCW flow reactor at 450−500 °C and 30 MPa were studied by TEM. TEM image displayed in Figure 4 indicates that the Ba-hexaferrite nanocrystals with an unmodified surface possesses platelike irregular shape particles with an average diameter of 28 nm and the particles were aggregated (Figure 4e). When the oleic acid (molar ratio to Ba-hexaferrite precursor 10:1) was supplied to the reaction system, the nano cube shape particles formed with an average particle size of 9 nm (Figure 4a). As the concentration of the oleic acid was increased (molar ratio to Ba-hexaferrite precursor 50:1), the shape of the Ba-hexaferrite nanocrystals was transformed to octahedral shape with an average size of 8 nm (Figure 4b). These nanocrystals exhibit a self-assembled 2D array on the surface of carbon coated copper grid with a nearest-neighbor spacing of ca. 4 nm by oleic acid capping group. The histograms of the particle size distribution analyzed by the transmission electron micrographs is plotted as shown in

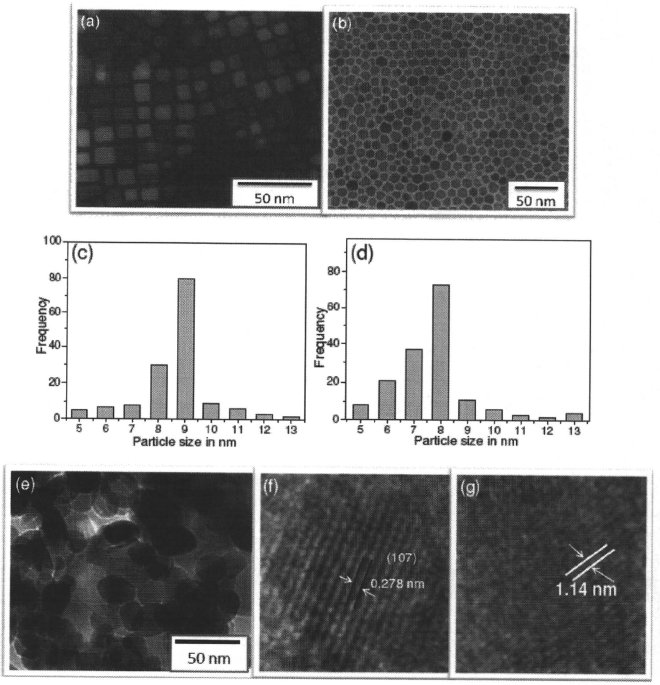

Figure 4. TEM images of the Ba-hexaferrite nanocrystals. The molar ratios of oleic acid to $BaFe_{12}OH_x$ precursor were (a) 1:10, (b) 1:50, (e) 1:0. (c) and (d) are histograms of the particle size distribution analyzed from (a) and (b), respectively, (f and g) well resolved lattice plane of the selected particle in (b and a).

Figure 4c,d. These data are consistent with DLS and XRD data. The single-crystallinity and structure of the synthesized sample was further confirmed by HRTEM. Distinct lattice planes in the HRTEM image further suggests that the particles obtained are single crystals, and particle shows a well resolved lattice plane with an interplanar spacing of 0.278 nm corresponding to the [107] plane of the hexagonal structure (Figure 4f) with $P6_3/mmc$ (194) space group, which was identified on the basis of data from the standard Ba-hexaferrite database JCPDS file, No. 39-1433. The HRTEM analysis for the cubes was carried out, which were oriented perpendicular to the *c* direction, in order to find that they are cubes but not the platelets lying on the basic plane. In general, the cubes of the hexaferrite structure were expected to have the dominant periodicity that corresponds to half of the cell parameter along the *c*-direction (002). It was difficult to find the cubes, which were oriented perpendicular to the *c* direction on the HRTEM grid. However, we found a few such particles and confirmed that they exhibit a lattice fringe with a distance of 1.14 nm as shown in Figure 4g. The nanocrystals synthesized in the presence of organic ligand showed a pronounced effect on the size and morphology of the nanocrystals indicating the capping effect on nanocrystals. In this way, we could prepare the organic ligand capped nanocrystals in a short reaction time of about < 1 min by controlling the growth process, which tends to take place at a long reaction time otherwise.[4] This results in the shape- and size-controlled formation of Ba-hexaferrite colloidal nanocrystals. Very recently, Primc et al. have used oleic acid as a stabilizing and growth controlling agent for the synthesis of ultrafine Ba-hexaferrite nanoparticles, under mild hydrothermal conditions.[13a] However, the size- and shape-controlled synthesis of Ba-hexaferrite nanocrystals are rarely reported, as not many researchers have focused on the use of organic ligand during the Ba-hexaferrite nanocrystal preparation. These findings should open new ways to tailor the size- and shape-controlled Ba-hexaferrite nanocrystals for their applications, for example, in high density magnetic memory devices.

Magnetic Property. The magnetization versus magnetic field plot at 5 and 280 K for Ba-hexaferrite nanocrystals capped with organic ligand is shown in Figure 5. The saturation magnetization of Ba-hexaferrite nanocrystals, measured at a maximum applied magnetic field of 60 kOe is about 19 and 14 emu/g at 5 and 280 K, respectively. These are lower than the values reported by other investigators using different preparation techniques 30−40 emu/g.[14] Actually, it is a well-known fact that the saturation magnetization decreases with the decrease in particle size of the magnetic materials. This is due to many